Flow changes due to pathologies of the left ventricle

Federico Domenichini[1], Gianni Pedrizzetti[2]
[1]*Department of Civil and Environmental Engineering, University of Firenze, Italy*
E-mail: federico.domenichini@unifi.it

[2]*Department of Civil and Environmental Engineering, University of Trieste, Italy*
E-mail: giannip@dica.units.it

SUMMARY. The diagnostic process in cardiology is primarily based on the study of the myocardial mechanics. The blood dynamics inside of the cardiac chambers is still an open issue, and it is rarely used in the clinical practice. The flow in an idealized left ventricle is here analyzed for akinetic and dyskinetic myocardial motion corresponding to the presence of an ischemic pathology. The study is performed with the numerical solution of the three-dimensional equations governing the flow. The results show that an anterior-inferior wall infarction leads to the shortening and weakening of the diastolic mitral jet. The diminution of the wall mobility is related to a region of stagnating flow close to the ischemic segment, in agreement with clinical findings. The detected phenomena are also noticeable for moderate degrees of the pathology. This suggests a potential value of the physically-based study of the patho-physiological intraventricular flow to develop early diagnostic indicator.

1   INTRODUCTION

The left ventricle (LV) is the most important chamber of the human heart, the lack of its contractility reflects immediately into the availability of oxygenated blood in the whole body and it can give rise to symptomatic pathologies, up to cardiac arrest. A dysfunction of the systolic phase, the contraction of the ventricle with the ejection of blood in the primary circulatory system, is often preceded by a weaker, possibly asymptomatic, diminution of efficiency that is more difficult to detect, and whose identification represents a challenge to physicians [1]. Diagnosis at the early stage of a pathology represents a central issue in cardiology. An early detected dysfunction can be controlled by a light pharmacological therapy. Pathologies discovered at an advanced stage may produce irreversible modifications or could require invasive approaches. It is therefore important to seek for a deeper understanding of the LV mechanics in patho-physiological conditions. And to develop schemes for the description of the differences that can be observed, and eventually to employ them for the physically-based improvement of the diagnostic techniques.

This study is focussed on the regional LV ischemia and its relation with the intraventricular fluid dynamics. Ischemia is a one of the most important systolic dysfunction due to the partial or total occlusion of a coronary vessel, which leads to the decrease of blood perfusion in the myocardial tissue. By a mechanical point of view, an ischemic portion of the ventricular wall has a reduced contractility and a progressive akinetic behavior, when it is passively transported by the closest segments. The result of an important or long lasting ischemic pathology is dyskinesia. The pathologic segment moves in the direction opposite to that of the other ones, because the tissue has locally lost its functionality and the segment tends to expand during the systolic contraction because of the pressure increase in the ventricle. It is worth to notice that, given the periodicity of the heart cycle, an abnormal behavior during systole is likewise reflected during the diastolic phase. A dyskinetic

segment that moves outward during the contraction necessarily displaces inward during the diastole [2].

The diagnosis of the cardiac function is mainly based on the evaluation of the tissue motion with medical imaging techniques like Magnetic Resonance Imaging (MRI) and echocardiography. Global indexes (like the Ejection Fraction, EF) are routinely estimated, and they give a measure of the pumping efficiency of the LV. The segmental LV contractile strength has been initially evaluated by measuring the thickening of the tissue and its inward motion (M-mode echocardiography) and, more recently, by measuring the myocardial strain by tissue Doppler echocardiography, tagged-MRI, or, lately, 2D-strain techniques. These methods allow, within some limitations, to quantify the regional activity of the myocardium with good accuracy and reproducibility. On the other side their application in the clinical practice is still under discussion.

The purpose of LV work is to give an efficient propulsion to the blood. The intraventricular fluid dynamics is therefore directly related to the LV functionality, and its study may furnish additional information useful to the diagnostic process. The flow in the left ventricle shows a peculiar arrangement due to the development of vortices [3, 4] that are influenced by the motion of the surrounding boundary (endocardium). In normal cases, the flow has an asymmetric vortex structure that allows an efficient diastolic filling [5, 6], and a natural redirection toward the aortic outflow [7]. Theoretical studies have shown the potential development of changes of the intraventricular flow in presence of specific pathologies [8, 9], and the close relation between the asymmetry of the mitral inflow and the global efficiency of the LV work [10]. Some aspects of the cardiac fluid mechanics has been clarified by these studies, and by other ones cited therein. Nevertheless, the influence of the pathologies on the intraventricular flow is far from being completely explained, and further studies are necessary to give an actual contribute to the clinical phase.

Recent progresses of the imaging processing techniques have shown the possibility to visualize the intraventricular vortical flow [11, 12, 13]. On the other side, these results have clarified that their accurate interpretation necessarily must be supported by fluid dynamical concepts, with a interdisciplinary work aimed to explain, at least qualitatively, the influence of specific pathologies. In fact, flow visualizations are still of little usage in diagnosis. In the seminal paper [14] the intraventricular vortex flow was visualized with innovative, for that time, techniques, showing that with growing ischemia the vortical structure is increasingly unable to penetrate the ventricle. The resulting stagnating flow near the apex was suggested as the mechanism for thrombus formation in myocardial infarction.

Following [14], this work analyzes the left ventricular flow in presence of ischemia as provoked by the partial and total occlusion of the anterior descending coronary artery. The fluid dynamics is studied by mean of numerical simulations on artificially designed ventricles. The main objective is to give a physically-based evidence of the changes of the intraventricular flow from healthy state to controlled ischemic condition.

2   MATHEMATICAL MODEL AND NUMERICAL METHOD

The left ventricle wall presents a significant variability among individuals. On the other side, the details of specific geometries are not relevant when looking for phenomena with a certain degree of general validity. With this in mind, we consider here a simple geometry that can be assumed as a sort of average representation of the endocardial shapes. A healthy left ventricle is therefore described as half of a prolate spheroid. The motion of the cavity wall is given by the temporal variation of the LV height, $H(t)$, and of the diameter of its equatorial plane, $D(t)$, t is the time. The instantaneous ventricular volume is $V(t) = \frac{\pi}{6} H D^2$, the entering/exiting discharge $Q(t) = dV/dt$. In the healthy

2

case, the wall motion is completely specified from $H(t)$ and $D(t)$ [15, 6]. The blood is assumed to be a Newtonian incompressible fluid, whose dynamics is governed by the Navier-Stokes and continuity equations

$$\frac{\partial v}{\partial t} + v \cdot \nabla v = -\frac{1}{\rho}\nabla p + \nu \nabla^2 v,$$

$$\nabla \cdot v = 0,$$

$$(1)$$

v and p are the velocity and the pressure, $\rho = 1060\ kg/m^3$ and $\nu = 3.3\ 10^{-6}\ m^2/s$ are the density and the kinematic viscosity, respectively. The system (1) must be completed with the boundary conditions. The no-slip condition is enforced at at the cavity wall. At the equatorial plane, $z = 0$, which corresponds to the region below the mitral and aortic orifices, the entering/exiting jets are reproduced imposing their velocity profiles [10]. The mitral entry-jet is here assumed with a blunt shape

$$v_z(x, y, z = 0) = V_0 \exp\left[-\left(\frac{(x - x_0)^2}{\sigma_x^2} + \frac{y^2}{\sigma_y^2}\right)^4\right],$$

$$(2)$$

$x_0 > 0$ is the center of the jet, σ_x and σ_y are a measure of its dimensions, the reference velocity V_0 is evaluated to allow flowing into the cavity the exact quantity of fluid required by the LV volume variation rate $Q(t)$. From (2) it follows that $y = 0$ is the plane passing trough the mitral and the aortic orifices, the posterior LV wall and the anterior intra-ventricular septum (IVS); it corresponds approximately to the apical 3 chamber (A3C) projection in echocardiographic imaging, see Fig.1. The reference healthy dynamics of the LV wall has been taken from the analysis of echocardiographic images of a young subject, with $EF = 55\%$, the temporal variation of the cavity volume is reported in Fig. 2.

The myocardial infarction is reproduced modifying the wall dynamics in order to mimic different degrees of occlusion of the left anterior descending coronary (LAD). This is obtained starting from the healthy case and progressively reducing the longitudinal and circumferential strain of the IVS at median-apical level. This region, Fig. 1, roughly corresponds to a circumferential sector in the range $\pi/2 < \theta < 7\pi/6$ in the lower half of the LV wall, where θ is the polar azimuthal coordinate. At each instant of time the healthy strains at every point of the wall are multiplied by a reduction coefficient

$$c(\eta, \theta) = 1 - A \exp\left[-\left(\frac{\theta - \theta_c}{2\theta_s}\right)^4 - \left(\frac{\eta - \eta_c}{2\eta_s}\right)^4\right],$$

$$(3)$$

where η is the spheroidal coordinate along the wall, ranging from $\eta = 0$ at the apex to $\eta = \pi/2$ at the base [15], see Fig. 1. Once the modified strain values are calculated, the pathologic geometry is evaluated starting from the tele-diastole (ECG R-wave), where strain is assumed zero as reference. The region influenced by the infarction is defined by (3) with center at $\theta_c = 5\pi/6$ and $\eta_c = \pi/8$, and extension $\theta_s = \pi/3$ and $\eta_s = \pi/10$; an annular extension has been assumed for the longitudinal strain only to avoid LV tilting. The factor A represents the entity of the infarction: small values, $A < 1$, simulate a reduced wall motion. Values little larger than 1 correspond to a regional akinesia, higher ones to dyskinetic motion. Variations of A in the range $1 - 2$ give values of the EF from 45% to 32%.

The system (1) is solved in a computational box, with the LV boundaries immersed therein and taken into account through a version of the Immersed Boundary (IB) method [16]. Periodicity is
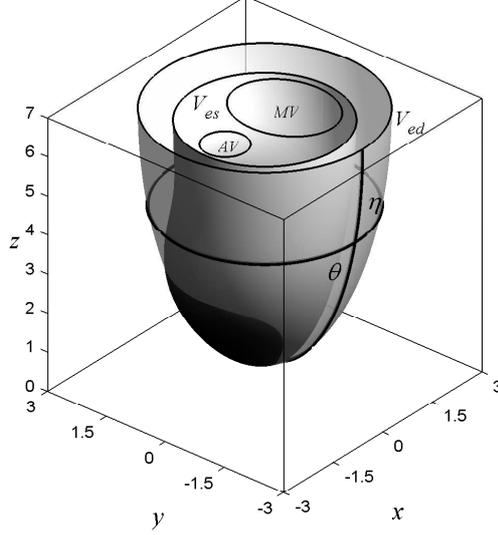
Figure 1: Sketch of the geometrical model. V_{es}= end systolic volume, V_{ed}= end diastolic volume, MV = mitral valve orifice, AV = aortic valve orifice. The spheroidal coordinates η and θ, equation 3, are also plotted. The darker area marks the ischemic region. Units are centimeters.

assumed along x and y, allowing the spectral representation of the variables and fast solution methods of the Poisson's problem for the mass conservation. Centered second-order finite differences on a three-dimensional staggered grid are employed for the temporal advancement of the Navier-Stokes equation, performed with a third order Runge-Kutta scheme. The velocity components are then transformed in their Fourier's representation, to compute the divergence and solve the Poisson's problem for the instantaneous irrotational correction of the pressure field [17]. With this method the $N_x \times N_y \times N_z$ Poisson's system is reduced to the solution of $N_x \times N_y/2$ tridiagonal linear systems of dimension N_z that can be achieved with a fast direct method. The corrections to the velocity and pressure fields are computed in the Fourier's space and transformed again in their physical counterparts.

The LV wall is represented by a two-dimensional mesh, in the η - θ space, whose at each time step are known both position and velocity. Any interpolation in used to impose the "inner" boundary condition at the wall, but the wall velocities are imposed to the closest point of the computational three-dimensional grid during the advancement of the Navier-Stokes equation [18]. The accuracy of the IB method and the choice of some numerical parameters have been verified by comparing the results with those obtained with a numerical code written in the body-fitted system of coordinates [6], showing almost undistinguishable solutions. The results here reported have been obtained with a computational grid $N_x = N_y = N_z = 128$. Several preliminary runs for the healthy case have been performed doubling the computational grid in all the directions to guarantee the convergence of the solution. The chosen grid has proven to be a good compromise between the convergence of the solution and the computational effort. The dimensions of the numerical box have been eventually set to $L_x = L_y = 6.6\ cm$, $L_z = 7\ cm$, the independence of the solution on the transversal
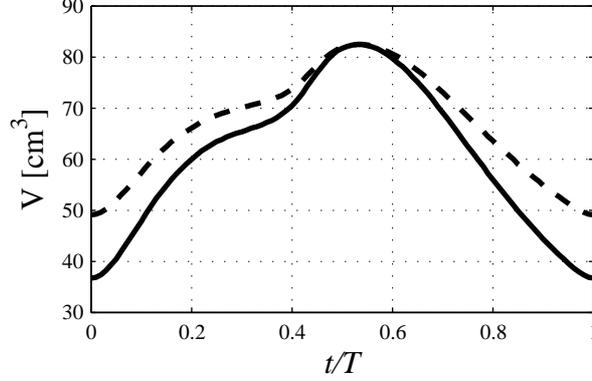
Figure 2: Volume of the cavity $V(t)$ for the healthy ventricle ($EF = 55\%$), continuous line, and for an ischemic ventricle with regional akinesia ($EF = 40\%$), dashed line

dimensions has been verified doubling L_x and L_y, showing a negligible influence of the assumption of periodicity. The time step of integration has been fixed to $\Delta t = T/1024$, being T the heartbeat period, to satisfy the stability conditions and accuracy of the unsteady IB approach [18].
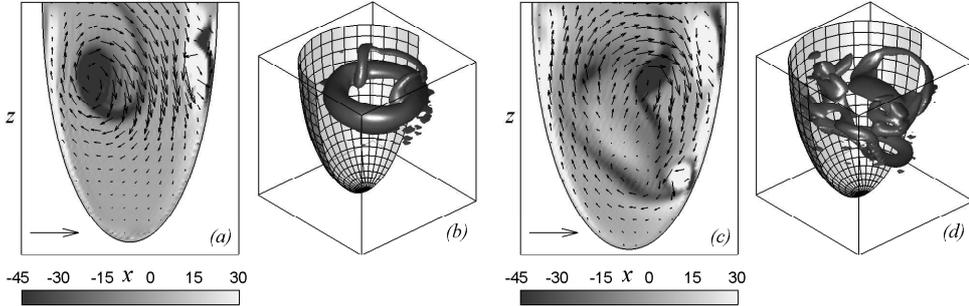

Figure 3: Flow in the left ventricle under healthy condition, $EF = 55\%$ at peak diastole (a) and (b) ($t/T = 9/32$), and during systole (c) and (d) ($t/T = 18/32$). Panels (a) and (c): Flow on the transversal plane across mitral and aortic orifices, distribution of the normal component of the vorticity field and on-plane velocity vectors. Vorticity values, s^{-1}, are shown in the color bars. Unit vector corresponds to $50\ cm/s$. Panels (b) and (d): Three-dimensional vortex structure visualized by isosurface of the λ_2 field, value $\lambda_2 = -450\ s^{-2}$.

3   RESULTS

The results are analyzed in terms of vorticity and velocity distributions on the plane $y = 0$ that crosses the mitral and aortic orifices, and in terms of the three-dimensional structure of the vorticity field identified by the so-called λ_2-method [19]. The normal case ($EF = 55\%$) is reported in Fig. 3. The velocity vectors are sampled from the finer computational grid to enhance the readability.
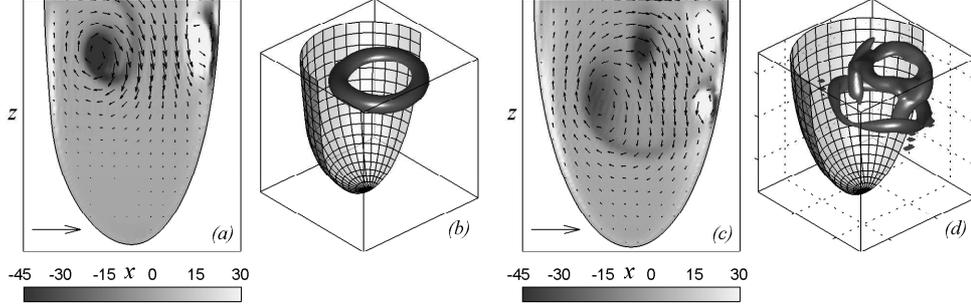
5

Figure 4: Flow in the left ventricle in moderate regional akinetic condition, $EF = 45\%$ at peak diastole (a) and (b) ($t/T = 9/32$), and during systole (c) and (d) ($t/T = 18/32$). Panels (a) and (c): Flow on the transversal plane across mitral and aortic orifices, distribution of the normal component of the vorticity field and on-plane velocity vectors. Vorticity values, s^{-1}, are shown in the color bars. Unit vector corresponds to 50 cm/s. Panels (b) and (d): Three-dimensional vortex structure visualized by isosurface of the λ_2 field, value $\lambda_2 = -450 \ s^{-2}$ and $\lambda_2 = -250 \ s^{-2}$, respectively.

During the early diastolic phase, the entering mitral jet develops a compact ring-shaped structure, whose two-dimensional cross-section is represented by two counter rotating vortices. The vortex on the anterior LV side (left in Fig. 3a,c) fills the central part of the chamber, the other (right) one creeps along the posterior wall and interacts with the boundary-layer. During the following evolution, the primary vortex structure deeply penetrates the ventricle, while a second structure, associated to the A-wave filling phase, say $0.4 \leq t/T \leq 0.5$, develops below the mitral plane. The primary structure shows a significant deformation, mainly due to the self-induced motion. In fact the left vortex tends to occupies the large part of the transversal section, while the right one is pushed toward the wall, where it is dissipated by the interaction with the opposite-sign boundary layer [6]. During the systolic contraction, the deformation of the structure leads to the complex three-dimensional field in Fig. 3d, which dissipates and it is finally ejected trough the aortic orifice.

The influence of a moderate reduction of the wall mobility ($A = 1$ in (3)), related to the diminution of the EF from 55% to 45%, can be observed in Fig. 4. The mitral jet penetrates less deeply the cavity and with lower levels of vorticity. As a consequence, the self-induced dynamics and dissipation are weaker, giving a more regular vortex structure at the end of the diastole, Fig. 4c and 4d. A more severe level of infarction, associated to a dyskinetic behavior ($A = 2$ in (3)), is reported in Fig. 5, where an increasingly shorter mitral jet can be observed. The large part of the ventricle is not affected by the vortex structures and by flow circulation. During the systolic phase, the flow redirected to the aortic outflow comes from the central and upper parts of the ventricle. Velocity is always almost null close to the apex, where the flow is nearly stagnating during the entire heart cycle.

A synthesis of the dominant circulatory pattern during the whole cycle is represented the steady-streaming flow, that is the flow averaged over the heartbeat period. It is shown from the healthy case, $EF = 55\%$ (Fig. 6a), to $EF = 45, 40, 32\%$ ($A = 1, 1.4, 2$ in equation (3)) in Fig. 6b-d. The dominant circulation, that characterizes the redirection of blood from the mitral inlet to the aortic orifice, becomes progressively shorter and weaker, while the stagnating area at the apex becomes more extended. The reduction of the jet length is related to the diminution of the EF as given by
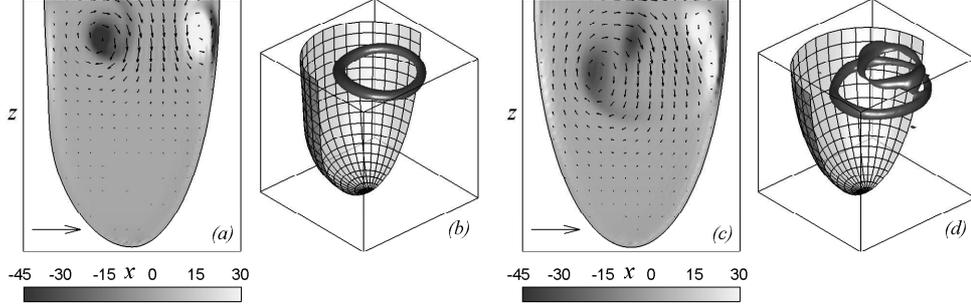
Figure 5: Flow in the left ventricle in regional dyskinetic condition, $EF = 32\%$ at peak diastole (a) and (b) ($t/T = 9/32$), and during systole (c) and (d) ($t/T = 18/32$). Panels (a) and (c): Flow on the transversal plane across mitral and aortic orifices, distribution of the normal component of the vorticity field and on-plane velocity vectors. Vorticity values, s^{-1}, are shown in the color bars. Unit vector corresponds to 50 cm/s. Panels (b) and (d): Three-dimensional vortex structure visualized by isosurface of the λ_2 field, value $\lambda_2 = -450 \ s^{-2}$ and $\lambda_2 = -200 \ s^{-2}$, respectively.

the simple calculation $L_{jet} = \int_{dia} Q dt / A_{MV} = (V_{ed} - V_{es})/A_{MV} = EF V_{ed}/A_{MV}$ from which it follows that the jet length, in first approximation, is proportional to the EF and

$$\frac{L_{jet}}{H_{ed}} = EF \frac{V_{ed}}{H_{ed} A_{MV}} \simeq EF \frac{\pi}{6} \frac{D_{ed}^2}{A_{MV}}. \tag{4}$$

This rough estimate assumes a one-dimensional unsteady jet that maintains a constant direction during the filling. In the present case, the jet also expands transversally, its shortening is further enhanced by the lateral motion at the base, because the small mobility at the apex reduces the capability of accommodating fluid therein.

4 CONCLUSIONS

The present work is focused on the influence of the reduced mobility of the myocardium, as caused by a LAD coronary stenosis, on the fluid dynamics inside of a left ventricle. To this aim, different degrees of ischemia have been simulated reducing progressively the mobility of the wall of an idealized ventricle cavity. The problem has been analyzed via numerical solution of the fluid dynamics equations.

Several simplifying assumptions have been made. Among these, the endocardial wall has been assumed to be smooth and the presence of the papillary muscles has not been taken into account. These factors would add disturbances to the wake structure, enhancing its dissipation, but are not expected to modify the global phenomenology. The idealized shape of the ventricle and the pathological motion of the wall have been defined artificially, rather than on the basis of clinical recordings. Thus, the results are focussed on the modification of the fluid dynamical pattern due to a specific pathology, but their actual relevance on the clinical practice is suggested but not demonstrated here.

Moreover, a held-open mitral valve has been considered, it does not take into account the leaflets dynamics, which can indeed modify the entry jet development. A previously tested inflow profile [6, 10], giving results in agreement with clinical studies [14, 11, 13], has been employed. In addition, a recent study on leaflet opening [20] partially supports this approximation showing that the vortex
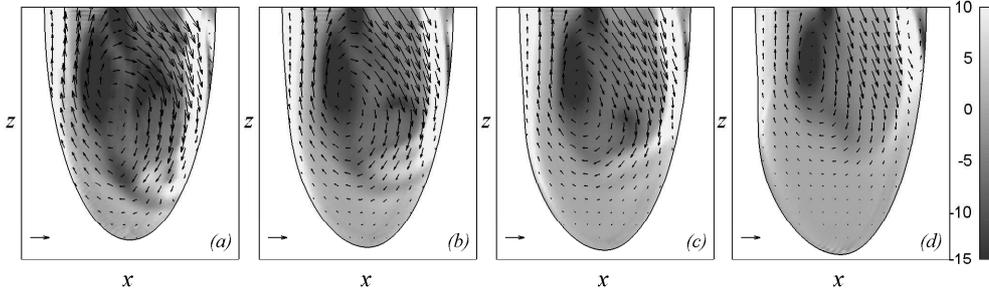
7

Figure 6: Steady streaming flow on the transversal plane across mitral and aortic orifices of the left ventricle in (a) healthy conditions ($EF = 55\%$), in (b) condition of moderate regional akinesia ($EF = 45\%$), (c) akinesia ($EF = 40\%$), and (d) relevant dyskinesia ($EF = 32\%$). Distribution of the normal component of the vorticity field and on-plane velocity vectors. Vorticity values, s^{-1}, are shown in the color bar. Unit vector corresponds to $10\ cm/s$.

from the longer leaflet (here the anterior) does not develop significantly until the leaflet reaches its final open position. In general, particular care must be used in modeling the transmitral flow for which limited information are available. At the present state of knowledge, it is not immediate to ensure a realistic modeling of the transmitral flow or, in alternative, of the leaflets geometry and their material properties. In this study, the simple entry flow model has been designed to give a realistic intraventricular flow and to reduce the impact of this issue. At the same time the possible modifications of the valvular dynamics due to the presence of a pathology are not addressed in this study that is focussed on the effect of the wall dyskinesia only.

Within the limitations of the present model, it has been shown that the ventricular wall infarction has a relevant impact on the flow dynamics. This is demonstrated by the shortening of the diastolic mitral jet, visualized by the lower intensity of the vorticity structure which characterizes the ventricular flow [3, 6]. Such effects are related to the diminution of the Ejection Fraction, that is closely related to the dimensionless length of the entering jet (4). The results give a physically-based explanation of the observations discussed in [14]. In addition, they show a stagnating fluid region close to the ischemic tissue, so that the vortex tends to keep away from that region.

It is worth to be noticed that such phenomena are already noticeable at moderately low level of disease. This suggests the potentiality of physically-based studies of the intraventricular flow for the development of early diagnostic indicators, either in normal and stress tests.

The results here presented have been obtained in an idealized geometry under controlled although simplified conditions. In presence of akinesia, and even more for dyskinetic behavior, the mitral jet enters less deeply inside the cavity. A stagnating region develops close to the wall segment with reduced mobility, where the fluid is not cleared out by the vortex structure created by the mitral inflow. These outcomes give a physical explanation to the phenomena that could realize in realistic physiological conditions, and encourage a clinical verification to progress in diagnostic methods based on the study of the flow dynamics.

References

[1] Wilson, P.W.F., D'Agostino, R.B., Levy, D., Belanger, A.M., Silbershatz, H. and Kannel, W.B., "Prediction of Coronary Heart Disease Using Risk Factor Categories," *Circulation*, **97**, 1837-1847 (1998).

[2] Sengupta, P.P., Korinek, J., Belohlavek, M., Narula, J., Vannan, M.A., Jahangir, A. and Khandheria, B.K., "Left Ventricular Structure and Function Basic Science for Cardiac Imaging," *J. Am. Coll. Card.*, **48**, 1988-2001 (2006).

[3] Kilner, P.J., Yang, G.Z., Wilkes, A.J., Mohiaddin, R.H., Firmin, D.N. and Yacoub, M.H., "Asymmetric redirection of flow through the heart," *Nature*, **404**, 759-761 (2000).

[4] Cooke, J., Hertzberg, J., Boardman, M. and Shandas, R., "Characterizing vortex ring behavior during ventricular filling with Doppler echocardiography: an in vitro study," *Ann. Biomed. Eng.*, **32**, 245-256 (2004).

[5] Cheng, Y., Oertel, H. and Schenkel, T., "Fluid-structure coupled CFD simulation of the left ventricular flow during filling phase," *Ann. Biomed. Eng.*, **33**, 567-576 (2004).

[6] Domenichini, F., Pedrizzetti, G. and Baccani, B., "Three-dimensional filling flow into a model left ventricle," *J. Fluid Mech.*, **539**, 179-198 (2005).

[7] Bolzon, G., Zovatto, L. and Pedrizzetti, G., "Birth of threedimensionality in a pulsed jet through a circular orifice," *J. Fluid. Mech.*, **493**, 209-218 (2003).

[8] Lemmon, J.D. and Yoganathan, A.P., "Computational modeling of left heart diastolic function: Examination of ventricluar dysfunction," *J. Biomech. Eng.*, **122**, 297-303 (2000).

[9] Baccani, B., Domenichini, F. and Pedrizzetti, G., "Vortex dynamics in a model left ventricle during filling," *Eur. J. Mech. B/Fluids.*, **21**, 527-543 (2002).

[10] Pedrizzetti, G. and Domenichini, F., "Nature optimizes the swirling flow in the human left ventricle," *Phys. Rev. Letters*, **95**, 108101 (2005).

[11] Sengupta, P.P., Khandheria, B.K., Korinek, J., Jahangir, A., Yoshifuku, S., Milosevic, I. and Belohlavek, M., "Left ventricular isovolumic flow sequence during sinus and paced rhythms," *J. Am. Coll. Card.*, **49**, 899-908 (2007).

[12] Hong, G.R., Li, P., Pedrizzetti, G., Domenichini, F., Wei, Z., Jin, S., Houle, H., Narula, J. and Vannan, M., "Impact of intraventricular blood flow vorticity on left ventricular function in normals and patients with heart failure: Quantitative assessment by contrast echocardiography using vector particle image velocimetry," *J. Am. Soc. Echocardiogr.*, **20**, 555 (2007).

[13] Hong, G.R., Pedrizzetti, G., Tonti, G., Li, P., Kim, J.K., Wei, Z., Houle, H., Jin, S., Narula, J., Chung. N. and Vannan, M., " Characterization and Quantification of Vortex Flow in the Human Left Ventricle by Contrast Echocardiography Using Vector Particle Image Velocimetry," *JACC Cardiov. Imaging*, **1**, 705-717 (2008).

[14] Beppu, S., Izumi, S., Miyatake, K., Nagata, S., Park, Y.D., Sakakibara, H. and Nimura, Y., "Abnormal blood pathways in left ventricular cavity in acute myocardial infarction. Experimental observations with special reference to regional wall motion abnormality and hemostatis," *Circulation*, **78**, 157-164 (1988).

[15] Baccani, B., Domenichini, F., Pedrizzetti, G. and Tonti, G., "Fluid dynamics of the left ventricular filling in dilated cardiomyopathy," *J. Biomech.*, **35**, 665-671 (2002).

[16] Mittal, R. and Iaccarino, G., "Immersed boundary methods," *Ann. Rev. Fluid Mech.*, **37**, 239-261 (2005).

[17] Verzicco, R. and Orlandi, P., "A finite-difference scheme for three-dimensional incompressible flows in cylindrical coordinates," *J. Comput. Phys.*, **123**, 402-414 (1996).

[18] Domenichini, F., "On the consistency of the direct forcing method in the fractional step solution of the Navier-Stokes equations," *J. Comp. Phys.*, **227**, 6372-6384 (2008).

[19] Jeong, J. and Hussain, F., "On the identification of a vortex," *J. Fluid Mech.*, **285**, 69-94 (1995).

[20] Pedrizzetti, G. and Domenichini, F., "Asymmetric opening of a simple bi-leaflet valve," *Phys. Rev. Letters*, **98**, 214503 (2007).